biophysica

MDPI

Article

A Novel Linear Evaluation of Chromatographic Peak Features in Pharmacopoeias Using an Inverse Fourier Transform Algorithm

Shuping Chen [1,2,*], Weiyuan Zhu [1], Sai Huang [2] and Baoling Zheng [2]

[1] Nexus Scitech Centre of Canada, 17 White Oak Crescent, Richmond Hill, ON L4B 3R7, Canada; charliezww@yahoo.ca
[2] Fujian Superimposegraph Co., Ltd., Floor 20-1402. 338, Hualin Road, Fuzhou 350013, China; sam@fjsuperimpose.com (S.H.); babaor@fjsuperimpose.com (B.Z.)
* Correspondence: shuping.chen@fjsuperimpose.com; Tel.: +1-416-638-4818

Abstract: The system suitability testing of chromatography is an indispensable procedure in pharmaceutical analysis, and it must comply with rules in related pharmacopoeias. An inverse Fourier transform algorithm was developed to accurately evaluate chromatographic features versus a standard Gaussian peak shape. The regular chromatogram is considered a pseudo-frequency spectrum and can be converted to a nominal time signal via inverse Fourier transformation. The system suitability parameters of peak width, theoretical plate number, tailing factor, and noise testing were evaluated using linear regressions directly and compared with the compendial rules. This novel method is simple, accurate, robust, reliable, and efficient for the evaluation of chromatographic peak features.

Keywords: chromatographic peak feature; system suitability; pharmaceutical analysis; inverse Fourier transform; Gaussian and distortion peaks

check for updates

Academic Editor: Matthias Buck

Received: 16 March 2025
Revised: 22 May 2025
Accepted: 29 May 2025
Published: 2 June 2025

Citation: Chen, S.; Zhu, W.; Huang, S.; Zheng, B. A Novel Linear Evaluation of Chromatographic Peak Features in Pharmacopoeias Using an Inverse Fourier Transform Algorithm. *Biophysica* **2025**, *5*, 21. https://doi.org/10.3390/biophysica5020021

Copyright: © 2025 by the authors. Licensee MDPI, Basel, Switzerland. This article is an open access article distributed under the terms and conditions of the Creative Commons Attribution (CC BY) license (https://creativecommons.org/licenses/by/4.0/).

1. Introduction

Pharmaceutical quality controls are closely related to therapeutical effects and public health. Various chromatographs are essential and principal equipment in analytical and research laboratories of pharmaceutical industries. System suitability criteria of chromatography ensure accuracy and reliability in chromatographic analysis. The important performance evaluations include the peak width, theoretical plate number, tailing factor, and resolution if more than one analytical component is present in the chromatogram. Highly pure standard substances are usually used in calibrations of chromatographic systems, and they must display good performance to meet the analytical criteria quantitatively and qualitatively. Their chromatographic peak shape should be outstandingly good and distinguishable with little interference. The ideal chromatographic peak shape was supposed to be a Gaussian profile [1]. This famous theorem has been used for more than eighty years and testified through modern chromatography and state-of-the-art developments in chromatographic column chemistry [2–15].

A regular chromatographic Gaussian peak can be written as a function of the elution time, t, and the standard deviation, σ [2] (pp. 217–224):

$$G(t - t_R) = A \exp(-[(t - t_R)/\sigma]^2/2),$$

where A is its intensity, and t_R is its retention time. Because of the full width at the half maximum (FWHM) of the Gaussian $W_h = \sqrt{8 \ln 2}\sigma$, the above equation is expressed with W_h:

$$G(t - t_R) = A \exp(-4\ln 2[(t - t_R)/W_h]^2). \quad (1)$$

In this work, we study system suitability parameters related to the chromatographic peak features: the peak width, theoretical plate numbers, and tailing (or symmetric) factor. It is mandatory to achieve a good peak shape with a high plate number in pharmaceutical analysis. According to the current harmonized pharmacopeia monograph [16] in the US pharmacopoeia (USP), European Pharmacopoeia, and Japan Pharmacopoeia, the plate number N should be calculated as follows:

$$N = 5.54\ (t_R/W_h)^2. \quad (2)$$

Since the system suitability tests are routinely performed with higher sampling rates, the retention time, t_R, of a peak generally can be precisely determined.

Markevich and Gertner compared five different methods to calculate FWHM for Gaussian or near-Gaussian profiles in 1989 [17]. The direct measurement of the FWHM is the most in use [16,17]. The second moment (variance) is also used to compute the FWHM of a chromatographic peak if the peak profile is exactly known [17]. However, chromatographic noises can affect all of these current methods. Taking a Gaussian profile as a reference (Gaussian paragon), we developed a novel inverse Fourier transform (FT) algorithm to linearly evaluate FWHM, as well as the plate number of a chromatographic peak, regardless of its real shape with highly denoising capability.

The method script is outlined below:

1. Purpose:

To evaluate equivalences of various tailing chromatogram peaks to fundamental Gaussian shape.

2. Generate a Gaussian profile as a chromatogram paragon with the same sampling rate of the system suitability test (better with similar peak height and width at half maximum to the analyzed peak).

3. Apply inverse Fourier transform for the Gaussian paragon versus nominal time to get its exponential Gaussian envelope.

4. Take the logarithm of the Gaussian envelope $\ln|\text{envelope}|$, and then perform a linear regression of $\ln|\text{envelope}|$ against square of nominal time to obtain its slope (R-square $\equiv 1$).

5. Apply the same procedures for the analyzed peak as above Gaussian paragon: inverse Fourier transform, logarithm of exponential envelope and linear regression to obtain the slope of the analyzed peak with a proper R-square criterion (for example, R-square ≥ 0.995).

6. Calculate the equivalent Gaussian peak width of the analyzed peak from their slope ratio regarding the Gaussian paragon width. The chromatographic plate number corresponding to the Gaussian paragon can be evaluated as per the pharmacopoeia formula.

2. Materials and Methods

2.1. Chemical Reagents and Solution Preparation for Gas Chromatography

Reagents used in this study: Methanol and n-Hexane, HPLC-grade from Sigma-Aldrich (Nanjing, China); Dimethyl Sulfoxide, HPLC-grade from Nanjing Chemical Reagent (Nanjing, China). The standard solution for gas chromatographic analysis was prepared through the procedure below. Accurately transfer 240 µL of Methanol and 27 µL of n-Hexane into a 50 mL volumetric flask nearly filled with Dimethyl Sulfoxide. Dilute to volume with Dimethyl Sulfoxide (stock standard solution). Transfer 4.0 mL of the stock standard solution into a 100 mL volumetric flask half-filled with Dimethyl Sulfoxide, and then

dilute to volume with Dimethyl Sulfoxide (working standard solution). Transfer 2.0 mL of the working standard solution into a 10 mL headspace vial (analytical solution) for the headspace sampler. The working standard solution contained 0.15195 mg/mL of Methanol and 0.01426 mg/mL of n-Hexane (calculated with density of Methanol = 0.7914 g/mL and density of n-Hexane = 0.660 g/mL).

2.2. Fourier Transform Methods in Chromatography

Despite the fact that the individual components are analyzed regarding their retention times in column chromatography, the chromatogram is the output measurements recording separations of individual components, similar to a spectrum in spectroscopy. The FT algorithm had been introduced to chromatography more than five decades, mainly for peak sharpness and noise suppression [18]. The signal truncations in FT induce the Gibbs effect (side-lobes) to the spectral peaks and should be apodized with a proper window function [18]. Therefore, the recovered chromatographic peaks with FT are not genuine ones. Wahab and his colleagues recently initiated several novel approaches to evaluate total chromatographic peak shape rationally matching a Gaussian profile (for example, above an 80% peak height) [19–21]. They further used inverse FT algorithms to sharpen chromatographic peaks and deconvolute highly overlapped peaks when the peak shape tailing was determined [22]. Alternatively, we use inverse FT to measure peak widths and plate numbers of any chromatographic peak versus a Gaussian paragon as long as they are yielded at the same sampling rate.

If a signal, $f(t)$, is a function of time, t, its FT spectrum, $F(v)$, in a frequency domain, v, (angular frequency $\omega = 2\pi v$) is commonly written as follows [18,23]:

$$F(v) = \int_{-\infty}^{\infty} f(t)\ \exp(-i2\pi vt)dt, \tag{3}$$

where $i = \sqrt{-1}$, and the exponential function $\exp(-i2\pi vt)$ is the kernel of FT. The inverse FT of $F(v)$ is defined to be as follows:

$$f(t) = \int_{-\infty}^{\infty} F(v)\ \exp(i2\pi vt)dv. \tag{4}$$

We presume that a chromatogram based on the retention time is equivalent to a spectrum in frequency. Thus, the inverse FT can be performed for the chromatogram peaks. For a Gaussian function, $G(t - t_R) = A\ \exp[-\alpha\pi(t - t_R)^2]$, its inverse FT should be as follows [23]:

$$g(t') = \int_{-\infty}^{\infty} A\ e^{-\alpha\pi(t\ -\ t_R)^2} e^{i2\pi t' t} dt = \frac{A}{\sqrt{\alpha}} e^{i2\pi t'\ t_R} e^{-\pi t'^2/\alpha}, \tag{5}$$

where t' is a nominal time in above inverse FT to distinguish the retention time, t, routinely used in chromatography. The retention time, t, represents a "location" in a chromatogram, corresponding to frequency, v, in spectroscopy. As per Equation (1), $\alpha\pi = 4\ln 2/{W_h}^2$. Following Euler's relation, $\exp(iz) = \cos(z) + i\ \sin(z)$ [18], the inverse FT of the Gaussian peak $G(t - t_R)$,

$$g(t') = A\sqrt{\frac{\pi}{\ln 2}}\frac{W_h}{2}\exp\left[-(\pi\ W_h\ t')^2/4\ln 2\right]\left[\cos\left(2\pi t_R t'\right) + i\sin\left(2\pi t_R t'\right)\right]. \tag{6}$$

The function $g(t')$ in the nominal time domain is a sinusoidal signal with real $\cos(2\pi t_R\ t')$ and imaginary $\sin(2\pi t_R\ t')$, which are a Hilbert-transform pair in Fourier analysis [24].

Hilbert transform provides a shortcut to extract the wave envelope because the absolute value of a complex function, $|x + iy| = \sqrt{x^2 + y^2}$ and $\cos^2(2\pi t_R\, t') + \sin^2(2\pi t_R\, t') = 1$:

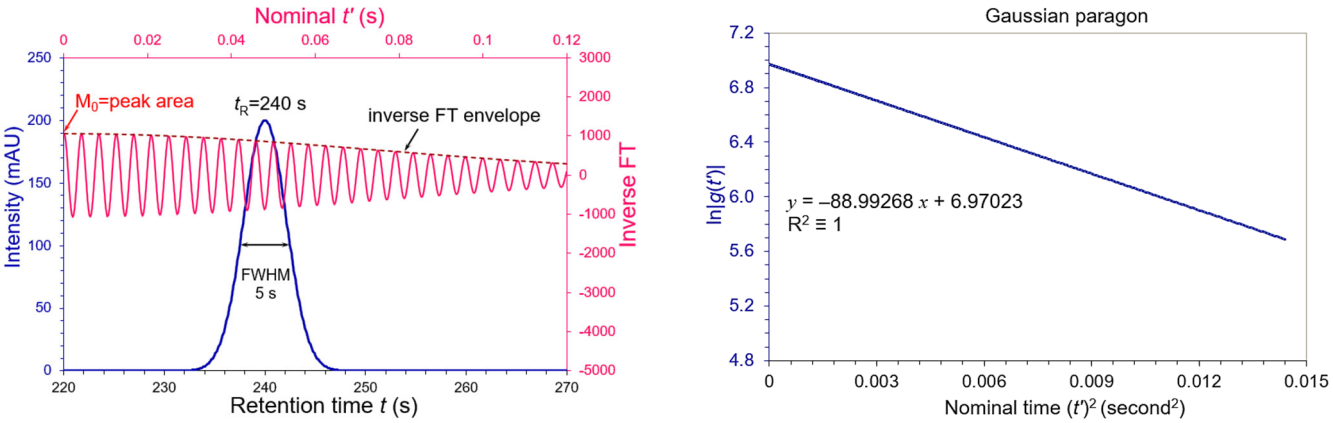
$$|g(t')| = A\sqrt{\frac{\pi}{\ln 2}}\frac{W_h}{2}\exp\left[-(\pi\, W_h\, t')^2/4\ln 2\right] \quad (7)$$

Taking a natural logarithm to both sides of Equation (7),

$$\ln|g(t')| = -\frac{(\pi\, W_h\, t')^2}{4\ln 2} + \ln\left[\frac{AW_h}{2}\sqrt{\frac{\pi}{\ln 2}}\right] = -K_G(t')^2 + \ln[M_0], \quad (8)$$

where $K_G = \pi^2 W_h{}^2/4\ln 2$, the Gaussian slope versus nominal $(t')^2$, and $\ln[M_0]$ is its intercept of the linear regression (zeroth moment M_0 = Gaussian peak area $AW_h\sqrt{\pi/4\ln 2}$).

A genuine Gaussian peak of liquid chromatography was simulated in Figure 1a by distributing 512 data points from 220 to 271.1 s (sampling rate = 10 Hz). We set the retention time t_R = 240 s, FWHM W_h = 5 s, and the peak height A_0 = 200 mAU. Its USP plate number = $5.54(240/5)^2$ = 12,764. When applying inverse cosine FT versus nominal t' lasting from 0 to 0.12 s, the Gaussian peak was converted to a sinusoidal $\cos(t_R\, t')$ (pink wave) with a Gaussian envelope (dash brown line), as shown in Figure 1a. A wellbeing outcome shown in Figure 1a is that the inverse cosine FT at nominal $t' = 0$ equals the zeroth moment M_0 = peak area ($AW_h\sqrt{\pi/4\ln 2}$) from Equation (8). We needed a distinctive feature of the Gaussian shape to compare with the other non-Gaussian shapes. This feature is the Gaussian slope K_G in Equation (8). According to the algorithm of Equation (6), we should use both the inverse cosine FT and the inverse sine FT to extract the envelope $|g(t')|$ and then implement linear regression on its natural logarithm $\ln|g(t')|$ versus the nominal $(t')^2$ (0–0.0144 s^2). Figure 1b is a perfect linear regression ($R^2 \equiv 1$) on the Gaussian envelope of Figure 1a. Its slope k_G ($=\pi^2 W_h{}^2/4\ln 2$) only relates to the peak width of the Gaussian peak. The linear regression data are all reported to five decimals.



(**a**) (**b**)

Figure 1. (**a**) A Gaussian shape (blue peak) was simulated as a chromatogram paragon (retention time t_R = 240 s; peak height A = 200 mAU; FWHM = 5 s at a sampling rate 10 Hz. Its inverse FT yielded a sinusoidal wave (pink wave) versus nominal time t' (secondary axes). The dashed brown line is its Gaussian envelope of the sinusoidal wave. The zeroth moment M_0 appeared at nominal time $t' = 0$ (indicated with a red arrow). (**b**) A linear regression for logarithm $\ln|g(t')|$ of the Gaussian envelope versus nominal $(t')^2$ from full 512 data points.

FTs are performed in discrete operations. The corresponding discrete FT formulations of Equations (3) and (4) are specified in the Appendix A section. Any commercial FT software will be suitable to evaluate the Gaussian envelope if the users have the initiative to the input frequency and time ranges. Because only a few hundred data points were

involved in the system suitability testing, it is very easy to implement the inverse FT in the Excel program, as shown in Section S1 of the "Supporting Information".

3. Results of Peak Width Evaluations

In the following simulation studies for non-Gaussian peak width evaluations, we always take a sampling rate 10 Hz because this rate (or higher) is sufficient to capture FWHMs of around 5 s. Meanwhile, the inverse FT was performed with 512 data points.

3.1. Symmetric Peaks

Absolutely symmetric peaks are seldom seen in chromatography. However, it is helpful to study non-Gaussian symmetric shapes first and understand how to compare non-Gaussian peaks to a Gaussian paragon. One outstanding symmetry is a centered Voigt shape. Theoretically, a Voigt peak is a convolution of Gaussian and Lorentzian distributions, involving a complicated integration form [25]. The Lorentzian shape $L(x)$ is a kind of spectroscopic peak from lifetime broadening or pressure broadening [25]:

$$L(x) = \frac{A}{1 + 4[(x - x_0)/W_h]^2}, \tag{9}$$

where A = peak height at position x_0, and W_h is FWHM of $L(x)$. Instead of using convolution integration, a pseudo-Voigt profile V_p, a linear combination of the Gaussian and Lorentzian, is a preferred approximation to represent centered Voigt peaks [19,25]:

$$V_p(\eta,\ t - t_R) = A\left\{\eta\ \exp\left[-\frac{4\ln 2(t - t_R)^2}{{W_h}^2}\right] + \frac{1 - \eta}{1 + 4[(t - t_R)/W_h]^2}\right\}, \tag{10}$$

where A is the peak height, and η is a contributing ratio between the Gaussian and the Lorentzian, $0 \le \eta \le 1$. We suppose that the Gaussian and the Lorentzian in Equation (10) have the same FWHM, W_h, and retention time, t_R.

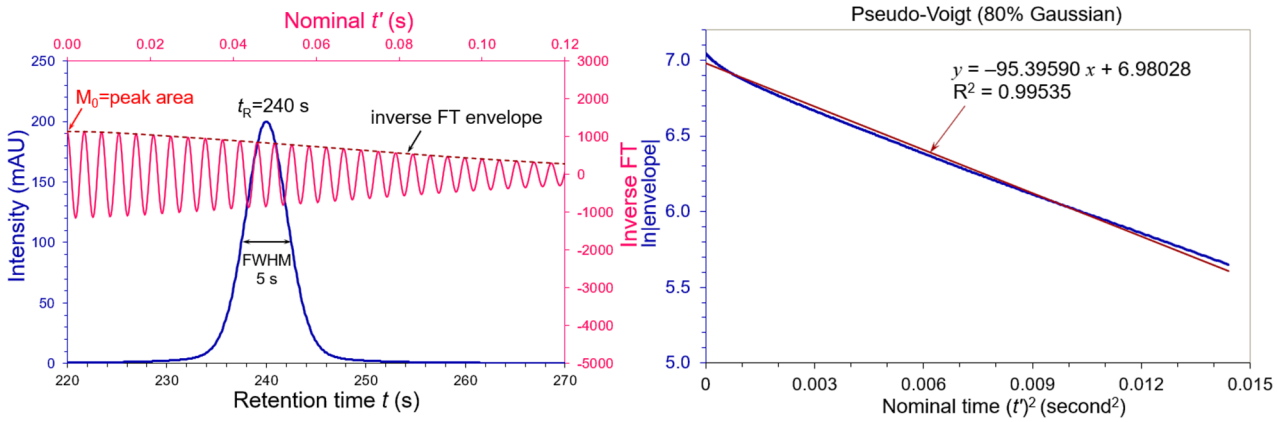
By setting η = 0.8 (80% Gaussian and 20% Lorentzian), a pseudo-Voight peak (blue peak) was simulated in Figure 2a using the exact same chromatographic parameters of the Gaussian paragon in Figure 1: t_R = 240 s, A = 200 mAU, and FWHM W_h = 5 s. The inverse cosine FT wave was depicted in pink and its envelope dashed brown. The ln | envelope | versus nominal $(t')^2$ in Figure 2b exhibited a good linearity with R^2 = 0.995. When comparing its slope K_S (=95.39590) in Figure 1 to slope K_G (=$\pi^2 {W_h}^2/4\ln 2$) of the Gaussian paragon, we deem its equivalent Gaussian FWHM W_{eG} to be as follows:

$$W_{eG} = W_h\ \sqrt{K_S/K_G}, \tag{11}$$

where W_h is the genuine FWHM of a Gaussian paragon. As K_G = 88.99268 (see Figure 1), the equivalent FWHM W_{eG} of this pseudo-Voigt peak is as follows:

$$W_h\sqrt{K_S/K_G} = 5 \times \sqrt{95.39590/88.99268} = 5.35976\,\text{s}.$$

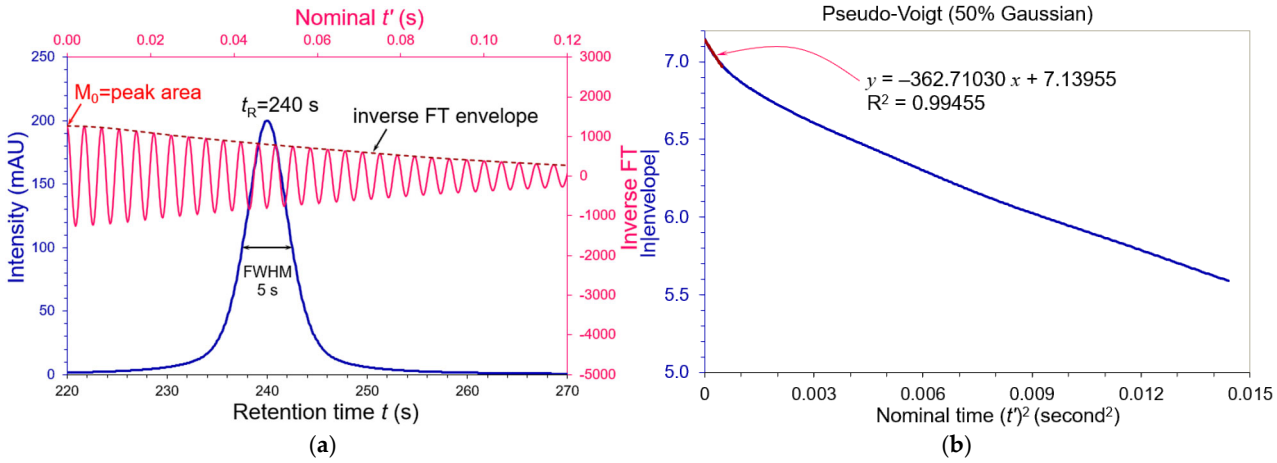
Its corresponding USP plate number $5.54(240/5.35976)^2$ = 11108. Although this pseudo-Voigt peak of 80% Gaussian component displayed the same FWHM W_h = 5 s in Figure 2a, its equivalent FWHM was actually increased by +7.2%, and the USP plate number dropped by −13% (against the plate number of the Gaussian paragon N = 12764).



(**a**) (**b**)

Figure 2. (**a**) A pseudo-Voigt peak of 80% Gaussian (blue peak) was simulated with the same chromatographic parameters as those in Figure 1. Its inverse FT sinusoidal wave was depicted in pink versus the nominal time t' (secondary axes) and its envelope in dashed brown. (**b**) A plot of logarithm ln | envelope | versus nominal, $(t')^2$. The trendline (solid brown) of the full 512 data points, $R^2 = 0.99535$.

Nevertheless, if the contribution ratio, η, continuously declined to 0.5 (50% Gaussian and 50% Lorentzian), the pseudo-Voigt peak displayed long tailings on both sides in Figure 3a and unfairly had the same USP plate number as the Gaussian paragon, according to Equation (2). A linear regression of ln | envelope | versus the nominal $(t')^2$ in Figure 3b bent upwards. Because the zeroth moment M_0 (peak area) must be included in the linear regression statistically, we demand that $R^2 \geq 0.995$ (accurate to 5 decimals) be an appropriate criterion to evaluate the similarity between a non-Gaussian shape and its Gaussian paragon. The first 94 data points of the inverse FT envelope exhibited linearity with $R^2 = 0.99455$ in Figure 3b.



(**a**) (**b**)

Figure 3. (**a**) A pseudo-Voigt peak of 50% Gaussian (blue peak). Its inverse FT sinusoidal wave was depicted in pink versus nominal time t' (secondary axes), and its envelope dashed brown. The zeroth moment M_0 at $t' = 0$ (indicated with a red arrow) must be included in the linear regression. (**b**) A plot of logarithm ln | envelope | versus nominal $(t')^2$. Its linear regression (solid brown) was performed for the first 94 data points, $R^2 = 0.99455$.

The pseudo-Voigt peak was not usually considered as a normal chromatographic peak [25]. Since the pseudo-Voigt peak has a distinct composition of the Gaussian component, it can be employed to theoretically examine the relation between the Gaussian percentage in a peak with the linear regression. Our study in Figure 2b indicated that the good linearity on the whole peak profile (full 512 data points) reached $R^2 \geq 0.995$ when

a peak was composed of an ≥80% Gaussian component. There is a turning point for the linearity performed on the full or partial envelope of its inverse FT as this R^2 criterion if the Gaussian component significantly drops below 80%, as shown in Figure 3b.

The slope K_S of the pseudo-Voigt peak with 50% Gaussian was determined to be 362.71030 in Figure 3b. Its equivalent FWHM as Equation (11):

$$W_{eG} = 5 \times \sqrt{362.71030/88.99268} = 10.09422\,\text{s}.$$

The corresponding USP plate number, $5.54(240/10.09422)^2 = 3132$. When the plate number, N, of this pseudo-Voigt peak was evaluated with the moments [10] (p.84) [19],

$$N = M_1{}^2/M_2 = 240^2/47.7159 = 1207, \quad (12)$$

where M_1 = the mean retention time, and M_2 = (total variance)^2. Obviously, the moments gave a more excessive N compared to our linear regression result. Such a long-tailing Voigt peak should not be acceptable in chromatographic analysis. It helps us build up the skills to evaluate substantial chromatographic peaks and their system suitability.

3.2. Asymmetric Peaks

The real chromatographic peaks are asymmetric, more or less, either fronting or tailing. The peak symmetry factor (also known as the tailing factor), as per USP [16], is as follows:

$$A_S = W_{0.05}/2d, \quad (13)$$

where $W_{0.05}$ is a peak width at 5% of the peak height, and d is the distance between the perpendicular dropped from the peak maximum and the leading edge of the peak at 5% of the peak height. There are many theoretical models to describe practical chromatographic peaks [2] (pp. 219–229) [21,25]. They generally convolute the Gaussian with another asymmetric profile, such as exponential tailing. The convolution is an accumulative result of shifting superposition regarding two or more real functions. We prefer to use the polynomial modified Gaussian (PMG) as a common model to describe asymmetric chromatogram peaks because it converges to the Gaussian shape when polynomial $\tau = 0$ [26,27]:

$$\text{PMG}(t - t_R) = A \exp\{-[y/(1 + \tau y)]^2\}, \quad (14)$$

where $y = 2(\sqrt{\ln 2})(t - t_R)/W_h$, and τ is a polynomial asymmetric factor. The W_h in the above equation is a theoretical FWHM of a Gaussian paragon, and it equals 5 s in the following simulation study.

A fronting PMG chromatographic peak at t_R = 240 s was simulated in Figure 4a by convoluting the Gaussian paragon in Figure 1a with a negative asymmetric factor, $\tau = -0.144$, which led its USP tailing factor, $A_S = 0.800$, and apparent FWHM = 5.07291 s. The pink wave is its inverse cosine FT, and the dashed brown line is the wave envelope. A linear regression of ln|envelope| versus nominal $(t')^2$ in Figure 4b covered the full 512 datapoints with a good $R^2 = 0.99832$ and yielded a slope of $K_S = 92.79001$. Its W_{eG} was calculated to be as follows:

$$5 \times \sqrt{92.79001/88.99268} = 5.10556\,\text{s}, \quad (15)$$

which is slightly different from the apparent FWHM 5.07291 s by +0.6%.

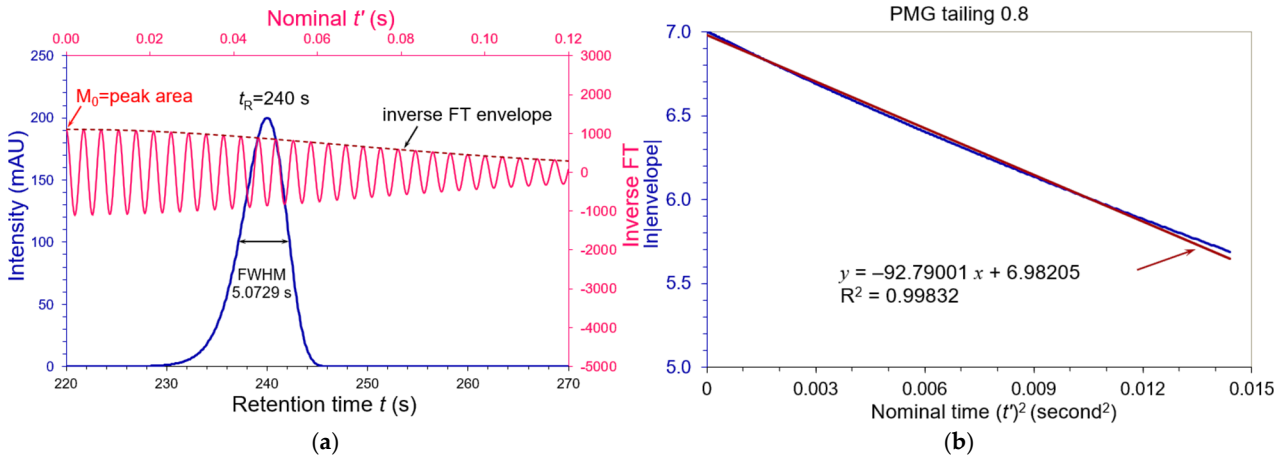


Figure 4. (**a**) A fronting PMG peak (blue peak: polynomial $\tau = -0.144$, USP tailing factor $A_S = 0.800$, and apparent FWHM = 5.07291 s) was simulated with the same chromatographic parameters as Figure 1. Its inverse FT sinusoidal wave was depicted in pink versus the nominal time t' (secondary axes), and its envelope is shown in dashed brown. (**b**) A plot of ln | envelope | versus the nominal $(t')^2$. Its trendline (solid brown) with the full 512 data points is $R^2 = 0.99832$.

We then simulated a tailing PMG peak at $t_R = 240$ s in Figure 5a with a USP tailing factor $A_S = 1.500$ and an apparent FWHM = 5.13209 s by shifting τ to positive + 0.1927. The pink wave in Figure 5a is its inverse cosine FT, and the dashed brown line is its envelope. A linear regression of full 512 data points by ln | envelope | versus the nominal $(t')^2$ was shown in Figure 5b, where slope *K*s = 95.17828 with $R^2 = 0.99481$ (barely met 0.995). Compared to the Gaussian paragon of Figure 1,

$$W_{eG} = 5 \times \sqrt{95.17828/88.99268} = 5.17085\,\text{s}.$$

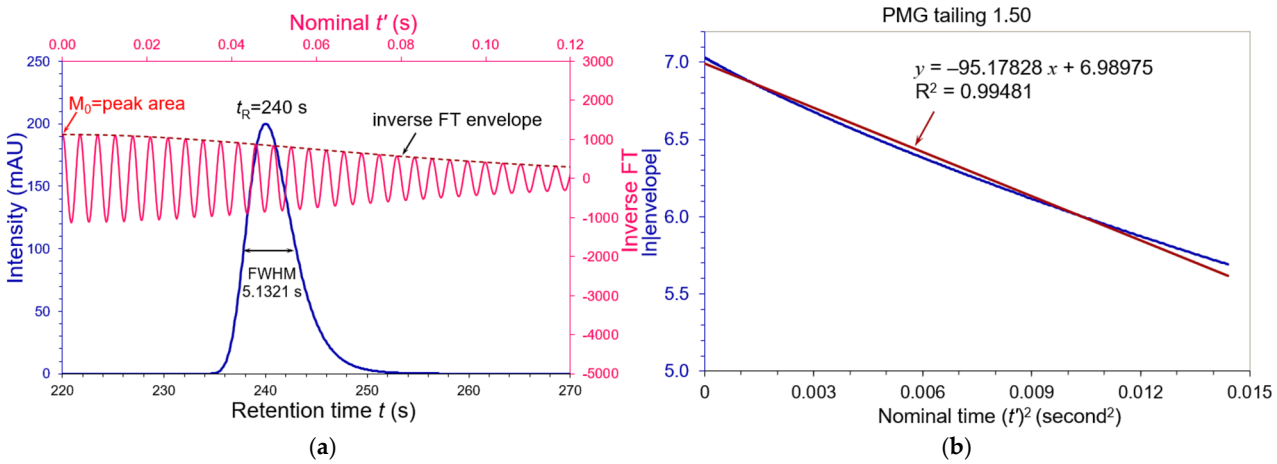


Figure 5. (**a**) A tailing PMG peak (blue peak: polynomial $\tau = +0.1927$, USP tailing factor $A_S = 1.500$, and apparent FWHM = 5.13209 s) was simulated with the same chromatographic parameters as Figure 1. Its inverse FT sinusoidal wave was depicted in pink versus the nominal time t' (secondary axes), and its envelope is shown in dashed brown. (**b**) A plot of ln | envelope | versus the nominal $(t')^2$. Its trendline (solid brown) with the full 512 data points of $R^2 = 0.99481$.

It was dilated by 0.7% relative to its apparent FWHM 5.13209 s.

It seems so far to have had little impact on the peak widths and plate numbers defined as the compendial criteria for the tailing factors within a range of 0.8 to 1.5. Let us extend our study to a peak tailing factor > 1.5. A very tailing PMG peak was formed in Figure 6a by convoluting the Gaussian paragon in Figure 1 with an asymmetric factor, $\tau = +0.2889$: USP

tailing factor A_S = 2.000 and FWHM = 5.30702 s. Using the same procedures, a linear regression of its ln | envelope | on the first 138 data points versus the nominal $(t')^2$ in Figure 6b yielded a slope K_S = 210.40537 with an R^2 = 0.99459. Its W_{eG} became the following:

$$5 \times \sqrt{210.40537/88.99268} = 7.68814\,\text{s}.$$

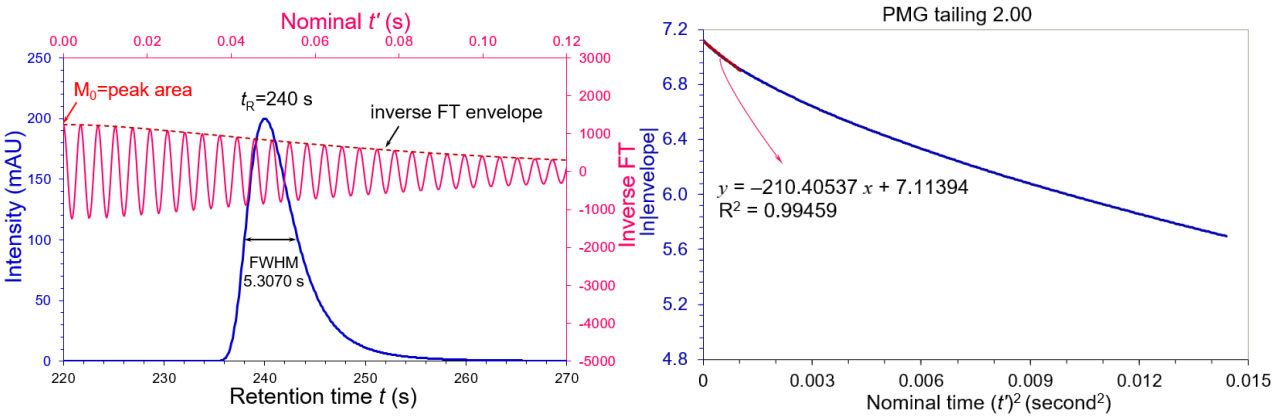


Figure 6. (**a**) A tailing PMG peak (blue peak: polynomial τ = +0.2889, USP tailing factor A_S = 2.000, and apparent FWHM = 5.30702 s) was simulated with the same chromatographic parameters as Figure 1. Its inverse FT sinusoidal wave was depicted in pink versus the nominal time t' (secondary axes), and its envelope is shown in dashed brown. (**b**) A plot of ln | envelope | versus the nominal $(t')^2$. The trendline (solid brown) of the first 138 data points of R^2 = 0.99459.

The dilation relative to its apparent FWHM = 5.30702 s achieved + 44.9%!

We summarized ten different tailing PMG peaks in Table 1 for their equivalent W_{eG} with USP tailings and compared their USP plate numbers with the W_{eG} plate numbers and moment plate numbers. The calculation details refer to S2 of the "Supporting Information". Since the fronting PMG peaks (A_S = 0.800 and 0.900) can be flipped horizontally to tailing peaks (A_S = 1.332 and 1.125), their flipped tailing peaks have the same peak widths and plate numbers. The N values evaluated with the W_{eG} in Table 1 are higher than those from moments $(M_1)^2/M_2$ because the moments statistically characterize pure mathematical distributions without comparing with a Gaussian paragon. Thus, our equivalent Gaussian width W_{eG} provides an appropriate measure of the peak width and plate number in chromatographic science. Please note that the deviation of W_{eG} from its apparent FWHM strongly depends on the peak shape. The deviation could be bigger or smaller if a chromatographic peak is other than a PMG shape with the same tailing factor. We will see a practical example in the application of gas chromatography.

Table 1. Tailings, FWHMs, equivalent W_{eG}, and plate numbers of ten PMG peaks.

Tailing A_S	FWHM (s)	W_{eG} (s)	N (USP)	N (W_{eG})	N (Moment)
0.800	5.07291	5.10556	12,400	12,242	10,357
0.900	5.01433	5.02384	12,691	12,643	12,273
1.125	5.01433	5.02384	12,691	12,643	12,333
1.332	5.07291	5.10556	12,400	12,242	10,477
1.500	5.13209	5.17085	12,116	11,935	8639
1.533	5.14405	5.24825	12,059	11,585	8274
1.571	5.15766	5.37839	11,996	11,031	7864
1.600	5.16822	5.47332	11,947	10,652	7549
1.750	5.22190	6.12634	11,702	8502	6047
2.000	5.30702	7.68814	11,330	5399	4178

3.3. Noise Testing of Peak Width Evaluation

Signal-to-noise ratio (SNR) is a very important attribute in the system suitability tests because it affects the quantitation limit and detection limit of a chromatographic method. The moment analysis also is very susceptible to noise [19]. Because FT has a great denoising capability in chromatographic analyses [18], our novel method offered a good solution to overcome the noise interferences in the measurements of the peak widths and the plate numbers using the inverse FT. Kotani et al. recently proved that the baseline noises in modern liquid chromatography followed normal distribution for a fixed UV detection wavelength [28]. Therefore, we generated white Gaussian noise in 512 data using a Python program (version 3.10.14) in Figure 7.

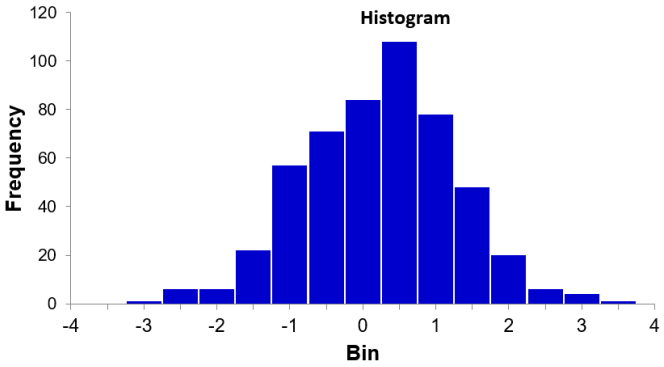


Figure 7. A histogram of a white Gaussian noise with Python 3.10.14 for the noise testing.

Since we formulated the linear regression slopes K_S or K_G as a function of FWHMs only, variations in the peak intensity will not affect the W_{eG} of a chromatographic peak. Our noise study was performed by proportionally adding the white Gaussian noise of Figure 7 to the tailing PMG peak in Figure 5 (USP A_S = 1.500) by reducing its intensity A_0 to 20 mAU at two different SNR levels: 10 and 20. We can feel the noise distortion from the chromatogram in Figure 8 at SNR = 10 (at the quantitation limit level). The noise made this PMG peak departure from the Gaussian more than the noise-free scenario and shifted its retention time t_R to 239.8 s. However, the noise only slightly influenced on linear regression slope of ln[envelope] versus the nominal $(t')^2$. For the linear regression slope = 96.79164 with R^2 = 0.99468 shown in Figure 8, its equivalent Gaussian W_{eG} was as follows:

$$5 \times \sqrt{96.79164/88.99268} = 5.21448\ s.$$

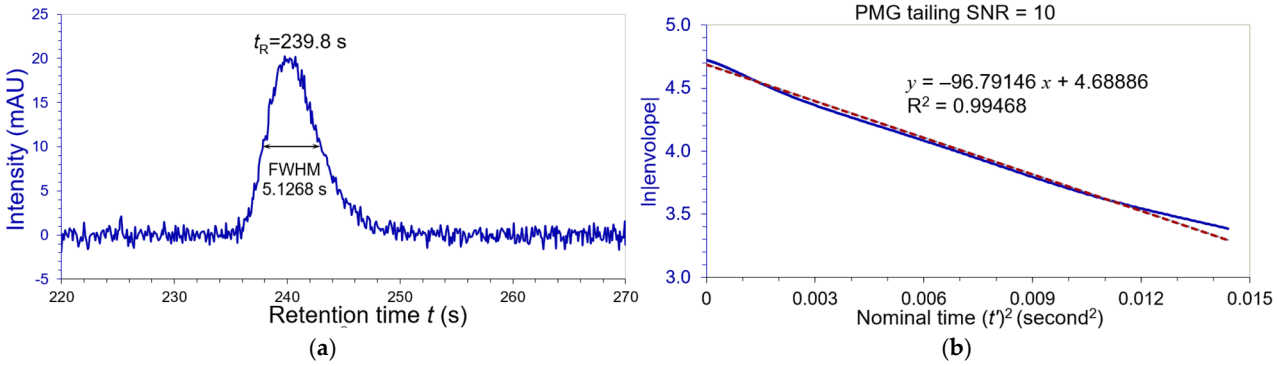


Figure 8. (**a**) The intensity of the tailing PMG peak in Figure 5 was reduced to 20 mAU and mixed with a white Gaussian noise at SNR = 10. Its retention time and FWHM were both affected. (**b**) A plot of ln | envelope | of the inverse FT versus the nominal $(t')^2$. The trendline (dashed brown) of the full 512 data points with R^2 = 0.99468.

Compared to the noise-free W_{eG} = 5.17085 s, this value was dilated only by +0.8%.

There was no doubt that the noise testing result of SNR = 20 can be better for the same tailing PMG peak. We found that its W_{eG} = 5.19288 s and the dilation was reduced to +0.4%. The inverse FT algorithm demonstrated a superior denoising capability. Therefore, the common baseline noises have little impact on the equivalent Gaussian peak widths using our inverse FT algorithm.

3.4. Application to Gas Chromatographic Analysis

Tests of residue solvents are routine analysis of drug substances and excipients used in pharmaceutical products. According to the USP monograph <467>, Methanol and *n*-Hexane both belong to Class II solvents with concentration limits of 3000 ppm and 290 ppm calculated from permitted daily exposure [16]. Figure 9a is a pure Methanol peak obtained from an Agilent 6890 II gas chromatograph with the following gas chromatography parameters: headspace injection, concentration = 0.15195 mg/mL of Methanol in Dimethyl Sulfoxide; SNR >500 at sampling rate = 10 Hz; carrier gas (Helium) flow rate = 1.6 mL/min; injector temperature = 180 °C; flame ionized detector temperature = 260 °C; J & W Scientific DB-624 30 m × 0.32 mm I.D., 1.8 µm film thickness; air = 340 mL/min, Hydrogen = 30 mL/min, auxiliary Helium = 28 mL/min; and oven temperature 40 °C for 5 min, then raised to 160 °C by a rate of 30 °C/min, and held for 2 min.

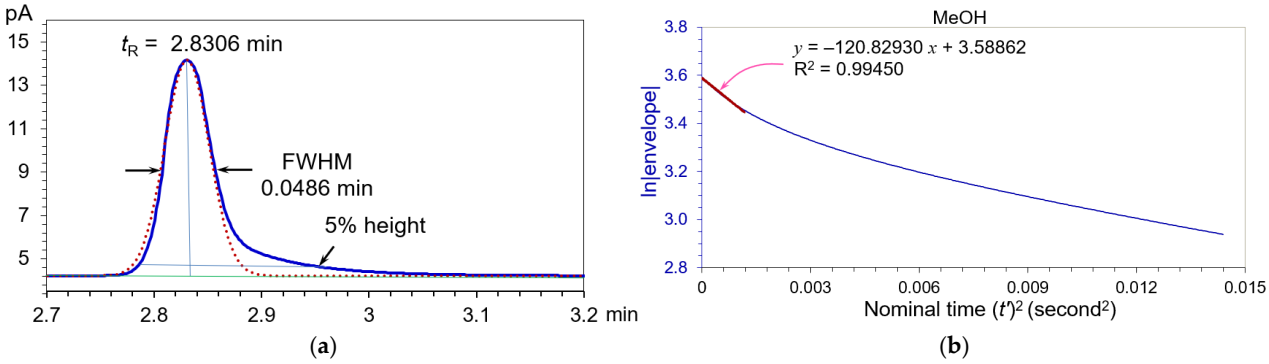


Figure 9. (**a**) The Methanol peak (blue peak) acquired from an Agilent 6890 II gas chromatograph at a retention time of 2.8306 min with an FWHM 0.0486 min. Its tailing factor (=1.747) was determined as per USP at 5% peak height. The dotted brown peak is its corresponding Gaussian paragon. (**b**) A linear regression of the inverse FT ln | envelope | versus nominal $(t')^2$ for the Methanol peak. The linearity of the first 147 data points (solid brown line) R^2 = 0.99450.

The Methanol peak in Figure 9a displayed a "fat" top at retention time 2.8306 min with an FWHM = 0.0486 min. Its USP tailing factor = 1.747 at one-twentieth of its peak height (5% height). By comparing it to the Gaussian paragon in Figure 9a (dotted brown peak, k_G = 30.28537) with the same peak height and FWHM, its equivalent Gaussian $W_{eG} = 0.0486 \times \sqrt{120.82930/30.28537} = 0.0971$ min from the K_S in Figure 9b. We calculated four kinds of its plate numbers: plate number N(tangent) = 21483, USP N(FWHM) = 18,813, $N(W_{eG})$ = 4708, and N (moments) = 3656. Therefore, the plate number for W_{eG} is a credible evaluation of the tailing Methanol peak.

Another residual solvent, *n*-Hexane (concentration = 0.01426 mg/mL), was simultaneously analyzed on the same gas chromatograph, and it demonstrated a nearly symmetric peak shape (blue peak) at a retention time of 6.5106 min in Figure 10 (FWHM = 0.0715 min with a USP tailing factor = 1.008). This *n*-Hexane peak almost coincided with its Gaussian paragon (dotted brown peak). As the above theoretical study, there is no need for the equivalent Gaussian analysis for tailing factors within 0.80 to 1.50.

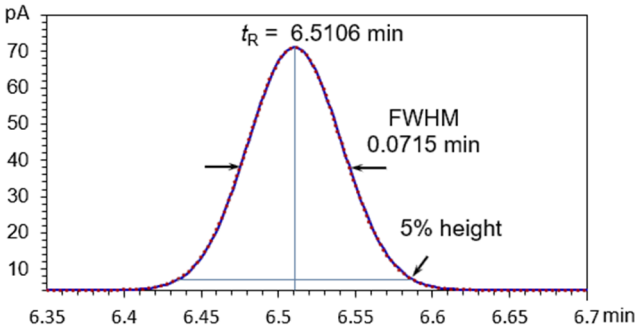


Figure 10. The *n*-Hexane peak (blue peak) analyzed simultaneously with the Methanol in Figure 9. Its t_R = 6.5106 min with an FWHM 0.0715 min and tailing factor = 1.008 at 5% the peak height. The *n*-Hexane peak matched well with a corresponding Gaussian paragon (dotted brown peak).

4. Discussion

We developed a novel approach to evaluating peak widths against a Gaussian paragon. Then, the plate numbers and resolutions in system suitability tests of pharmaceutical analysis could be calculated from the equivalent Gaussian peak width, W_{eG}. According to our theoretical studies on PMG tailing peaks, there is little influence on the peak widths for the peak tailing factors within 0.80 and 1.50. However, the equivalent Gaussian W_{eG} will gradually become wider when the USP tailing factor > 1.50 and cause significant deviations from the USP plate number and resolution if more than two peaks in a chromatogram. For example, the plate number could be reduced by −4% for a PMG peak with a tailing factor = 1.533 (see Table 1). When a peak has an extraordinary "fat" top, the equivalent Gaussian peak width W_{eG} could even be doubled like the Methanol peak shown in Figure 9. Any Gaussian shape can be employed as a paragon of a chromatogram as long as they are acquired by the same sampling rate with a sufficient SNR.

Individual enterprises always establish their own standard operation procedures according to regulatory guidelines laid down by related official authorities. We harbor no intention to challenge current pharmacopeias for the system suitability tests because there are many other system suitability attributes that conduct the controls to the extraneous variables. In particular, analytical procedure calibrations routinely employ reference standards in chromatographic analyses. To our best knowledge, in pharmaceutical analysis, optimization chromatographic methods must be robust. The peak tailing is usually controlled within 0.9 to 1.6 in method developments and validated corresponding appropriately to various chromatographic conditions, including intermediate precisions, adjustments of mobile phase(s), column temperature, flow rate, and system cleaning after complements of the analysis, etc. The reliability of a system suitability test strongly relies on the sampling rate used in chromatography. In this study, a sampling rate of 10 Hz was used for FWHMs of about 5 s. Our inverse FT method is very rugged to noise interference, even for SNR = 10, as long as the sampling rate is sufficient. If the sampling rate was lower than the optimal rate, SNR should be enhanced accordingly to compensation.

We laid out $R^2 \geq 0.995$ in the linear regressions to calculate the equivalent Gaussian peak width, W_{eG}, after extensively studying the simulated various tailing peaks. This value is adequate to compare any peak shape with a Gaussian paragon in the system suitability analysis. Nevertheless, the linear regression R^2 could be lowered slightly if it is too strict in some chromatographic analyses, depending on how to assess the similarity between the tailing peaks and Gaussian paragons. The inverse FT algorithm surmounts two major obstacles to directly comparing a chromatogram peak with the Gaussian paragon: the logarithm of negative baseline values and noise interferences.

With advances in modern chromatographic techniques, we should ensure the chromatographic methods are very repeatable and reproducible in pharmaceutical analysis.

That is, the chromatographic results, such as pharmaceutical assays, are highly precise with more than 95% confidence levels. Their variations are confined within small ranges. According to analytical quality by design principles in pharmaceutical industries, a chromatographic method should consistently perform well and be suitable for its intended use. The peak symmetry (or tailing), SNR (or noise variables), and resolution are included in "analytical procedure life cycle" (or called a "method life cycle management" of current USP [16,29]. Our novel inverse FT algorithm will be a credible approach to evaluating the system suitability attributes relating to peak features in the routine chromatographic methods developed and validated at different timelines and requirements.

The inverse FT evaluation of the spectral peak features also can be applied to other spectroscopic technologies. For example, the Gaussian is a fundamental peak shape in electrophoresis [30] and Gamma spectroscopy [31]. They are well-known analytical techniques in biochemistry and biomedicine.

5. Conclusions

Nowadays, countless chromatographs are running worldwide. Most of them are used for quantitative analysis, quality control, method validations, and technique transfers in pharmaceutical industries and biomedical research. In this work, we elucidated an inverse FT algorithm correlated with the Hilbert-transform envelopes to peak widths, the plate number for various tailing peaks in chromatography via linear regressions. The FWHMs and plate numbers are linearly evaluated versus the Gaussian paragons in the same sampling rate and regardless of their peak shapes. Our new approach was developed for routine chromatography used in pharmaceutical industries as per current pharmacopeias. Instead of directly measuring FWHM or full width at a 10% height $W_{0.1}$ with asymmetric factors A and B calculated as the Foley–Dorsey equation [32], the inverse Fourier transform algorithm demonstrated its advantage in plate-number evaluations. It is simple, accurate, robust, reliable, and efficient to improve the traditional evaluations of common chromatographic peak features in the global pharmacopeias.

Supplementary Materials: The following supporting information can be downloaded at https://www.mdpi.com/article/10.3390/biophysica5020021/s1: Excel S1: Inverse FT (512 datapoints); Table S1: Calculations of 10 PMG peaks.

Author Contributions: Conceptualization, S.C.; methodology, S.C.; software, S.H.; validation, B.Z., W.Z. and S.C.; resources, S.C. and B.Z.; data curation, S.C.; writing—original draft preparation, S.C.; writing—review and editing, W.Z. All authors have read and agreed to the published version of the manuscript.

Funding: This research received no external funding.

Data Availability Statement: All data analyzed during this study are included in this article.

Acknowledgments: We appreciate Zhuguang Lin, Department of Chemistry, Xiamen University, China, for the gas chromatogram in this work.

Conflicts of Interest: All authors have any potential interesting relations.

Abbreviations

The following abbreviations are used in this manuscript:

FT	Fourier transform
FWHM	Full width at half maximum
PMG	Polynomial modified Gaussian
SNR	Signal-to-noise ratio
USP	US pharmacopoeia

Appendix A

The discrete FT formulations of Equations (3) and (4) are expressed in a series of even N of data points for integers k or $m = -N/2+1, N/2, \ldots, 0, \ldots, N/2$:

$$F(k) = \sum_{m=-N/2+1}^{N/2} f(m)\ \exp(-i2\mathrm{km}/N), \tag{A1}$$

$$f(m) = \sum_{k=-N/2+1}^{N/2} F(k)\ \exp(i2\pi\mathrm{km}/N). \tag{A2}$$

For practical applications of the discrete FTs on chromatogram bands, the user should have the initiative to input frequency and time ranges into commercial FT software (such as Python, Matlab, or others) and make proper adjustments to fit the data lengths and the chromatogram sampling rates. Because only a few hundred data points were involved in the system suitability testing, an Excel program of the inverse FT was attached in Section S1 of the "Supporting Information".

References

1. Martin, A.J.P.; Synge, R.L.M. A new form of chromatogram employing two liquid phases: 1. A theory of chromatography. 2. Application to the micro-determination of the higher monoamino-acids in proteins. *Biochem. J.* **1941**, *35*, 1358–1368. [CrossRef] [PubMed]
2. Komsta, Ł.; Heyden, Y.V.; Sherma, J. (Eds.) *Chemometrics in Chromatography*; CRC: Boca Raton, FL, USA, 2018.
3. Dong, M.W. *HPLC and UHPLC for Practicing Scientists*, 2nd ed.; Wiley: Hoboken, NJ, USA, 2019.
4. Miller, L.M.; Pinkston, J.D.; Taylor, L.T. *Modern Supercritical Fluid Chromatography, Carbon Dioxide Containing Mobile Phases*; Wiley: Hoboken, NJ, USA, 2020.
5. Webster, G.K.; Kott, L. (Eds.) *Chromatographic Methods Development*; Jenny Stanford Publishing: Singapore, 2020.
6. Wan, Q.-H. *Mixed Mode Chromatography: Principles, Methods, and Applications*; Springer: Singapore, 2021.
7. Kromidas, S. (Ed.) *Optimization in HPLC, Concepts and Strategies*; Wiley-VCH: Weinheim, Germany, 2021.
8. Robards, K.; Ryan, D. *Principles and Practice of Modern Chromatographic Methods*, 2nd ed.; Academic Press: London, UK, 2021.
9. Poole, C.F. (Ed.) *Gas Chromatography*, 2nd ed.; Elsevier: Amsterdam, The Netherlands, 2021.
10. Moldoveanu, S.; David, V. *Essentials in Modern HPLC Separations*, 2nd ed.; Elsevier: Amsterdam, The Netherlands, 2022.
11. Stoll, D.R.; Carr, P.W. (Eds.) *Multi-Dimensional Liquid Chromatography, Principles, Practice, and Applications*; CRC: Boca Raton, FL, USA, 2022.
12. Hicks, M.B.; Ferguson, P.D. *Practical Application of Supercritical Fluid Chromatography for Pharmaceutical Research and Development*; Academic Press: London, UK, 2022.
13. Fanali, S.; Chankvetadze, B.; Haddad, P.R.; Poole, C.F.; Riekkola, M.-L. (Eds.) *Liquid Chromatography: Fundamentals and Instrumentation, Handbooks in Separation Science*, 3rd ed.; Elsevier: Amsterdam, The Netherlands, 2023; Volume 1.
14. Fanali, S.; Chankvetadze, B.; Haddad, P.R.; Poole, C.F.; Riekkola, M.-L. (Eds.) *Liquid Chromatography: Applications, Handbooks in Separation Science*, 3rd ed.; Elsevier: Amsterdam, The Netherlands, 2023; Volume 2.
15. Nesterenko, P.N.; Poole, C.F.; Sun, Y. (Eds.) *Ion-Exchange Chromatography and Related Techniques, Handbooks in Separation Science*; Elsevier: Amsterdam, The Netherlands, 2024.
16. General Chapters <621>, Chromatography; <467>, Residual Solvents, <1220> Analytical Procedure Lifecycle, The United States Pharmacopeia 49-NF 44. 2025. Available online: https://www.usp.org/ (accessed on 21 May 2025).
17. Markevich, N.; Gertner, I. Comparison among methods for calculating FWHM. *Nucl. Instrum. Methods Phys. Res. Sect. A* **1989**, *283*, 72–77. [CrossRef]
18. Felinger, A. *Data Analysis and Signal Processing in Chromatography*; Elsevier: Amsterdam, The Netherlands, 1998; pp. 19–39, 167–176.
19. Wahab, M.F.; Patel, D.C.; Armstrong, D.W. Total peak shape analysis: Detection and quantitation of concurrent fronting, tailing, and their effect on asymmetry measurements. *J. Chromatogr. A* **2017**, *1509*, 163–170. [CrossRef] [PubMed]
20. Misra, S.; Wahab, M.F.; Patel, D.C.; Armstrong, D.W. The utility of statistical moments in chromatography using trapezoidal and Simpson's rules of peak integration. *J. Sep. Sci.* **2019**, *42*, 1644–1657. [CrossRef] [PubMed]
21. Burk, R.J.; Wahab, M.F.; Armstrong, D.W. Influence of theoretical and semi-empirical peak models on the efficiency calculation in chiral chromatography. *Talanta* **2024**, *277*, 126308. [CrossRef] [PubMed]

22. Wahab, M.F.; Gritti, F.; O'Haver, T.C. Discrete Fourier transform techniques for noise reduction and digital enhancement of analytical signals. *TrAC Trends Anal. Chem.* **2021**, *143*, 116354. [CrossRef]
23. Howell, K.B. *Principles of Fourier Analysis*, 2nd ed.; CRC Press: Boca Raton, FL, USA, 2017; pp. 304–322, 359–363, 492–493.
24. Kito, K. *Digital Fourier Analysis: Advance Techniques*; Springer: New York, NY, USA, 2015; pp. 105–119.
25. Di Marco, V.B.; Bombi, G.G. Mathematical functions for the representation of chromatographic peaks. *J. Chromatogr. A* **2001**, *931*, 1–30. [CrossRef] [PubMed]
26. Torres-Lapasió, J.R.; Baeza-Baeza, J.J.; García-Alvarez-Coque, M.C. A model for the description, simulation, and deconvolution of skewed chromatographic peaks. *Anal. Chem.* **1997**, *69*, 3822–3831. [CrossRef]
27. Baeza-Baeza, J.J.; Ortiz-Bolsico, C.; García-Álvarez-Coque, M.C. New approaches based on modified Gaussian models for the prediction of chromatographic peaks. *Anal. Chim. Acta* **2013**, *758*, 36–44. [CrossRef] [PubMed]
28. Kotani, A.; Watanabe, R.; Hayashi, Y.; Machida, K.; Hakamata, H. Statistical reliability of a relative standard deviation of chromatographic peak area estimated by a chemometric tool based on the FUMI theory. *J. Pharm. Biomed. Anal.* **2024**, *237*, 115777. [CrossRef] [PubMed]
29. Borman, P.J.; Guiraldelli, A.M.; Weitzel, J.; Thompson, S.; Ermer, J.; Roussel, J.M.; Marach, J.; Sproule, S.; Pappa, H.N. Ongoing analytical procedure performance verification using a risk-based approach to determine performance monitoring requirements. *Anal. Chem.* **2024**, *96*, 966–979. [CrossRef] [PubMed]
30. Landers, J.P. (Ed.) Introduction to capillary electrophoresis. In *Handbook of Capillary and Microchip Electrophoresis and Associated Microtechniques*, 3rd ed.; CRC: Boca Raton, FL, USA, 2008; pp. 13–19.
31. Gilmore, G.; Joss, D. *Practical Gamma-Ray Spectrometry*, 3rd ed.; Wiley: Chichester, UK, 2025; pp. 130–133, 425–428.
32. Foley, J.P.; Dorsey, J.G. Equations for calculation of chromatographic figures of merit for ideal and skewed peaks. *Anal. Chem.* **1983**, *55*, 730–737. [CrossRef]

Disclaimer/Publisher's Note: The statements, opinions and data contained in all publications are solely those of the individual author(s) and contributor(s) and not of MDPI and/or the editor(s). MDPI and/or the editor(s) disclaim responsibility for any injury to people or property resulting from any ideas, methods, instructions or products referred to in the content.